

# Electronic band structure of silver-deficient hexagonal AgB<sub>2</sub>

I.R. Shein\*, N.I. Medvedeva and A.L. Ivanovskii

*Institute of Solid State Chemistry, Ural Branch of the Russian Academy of Sciences, 620219, Ekaterinburg, Russia*

Structural, cohesive properties as well as energy band structure of metastable hexagonal AgB<sub>2</sub> and silver-deficient borides Ag<sub>0.875</sub>B<sub>2</sub> and Ag<sub>0.750</sub>B<sub>2</sub> were investigated by means of the projected augmented wave method in the framework of the density functional theory (VASP package). We found that the density of states at the Fermi level for nonstoichiometric diborides is almost constant within a range of vacancy content up to 25%. The formation energy of metal vacancies in silver diboride is the least among all 4d metal diborides, i.e. for AgB<sub>2</sub> is possible to expect the wide homogeneity region.

\* E-mail: shein@ihim.uran.ru

PACS numbers:

After the discovery of superconductivity with T<sub>c</sub> ~ 39 K<sup>1</sup> in layered MgB<sub>2</sub>, there have been a lot of theoretical searches for the potential superconductors with high T<sub>c</sub> among other diborides MB<sub>c</sub> (M = Na, Be, Ca, noble and transition metals)<sup>2,3,4,5,6,7,8,9,10,11</sup>, see also review<sup>12</sup>. Among them the silver diboride (AgB<sub>2</sub>) was predicted to be promising system having the larger density of B2p  $\sigma$ -like states near the Fermi level<sup>4</sup> and electron-phonon coupling constant than MgB<sub>2</sub> and hence higher T<sub>c</sub> (~ 60  $\div$  70 K)<sup>7,8</sup>.

However the attempts to synthesize AgB<sub>2</sub> lead to inconsistent results. For the first time the synthesis of AgB<sub>2</sub> phase (space group P6/mmm, lattice parameters a = 3.00 and c = 3.24 Å) has been declared thirty years ago<sup>13</sup>. Further the different experimental routes were used<sup>14</sup> to obtain AgB<sub>2</sub> samples as a bulk and thin films; however all synthesized AgB<sub>2</sub> samples were unstable.

Quite recently the successful synthesis of silver boride thin films with nominal composition AgB<sub>2</sub> was performed by a pulsed laser deposition method<sup>15</sup> and sharp superconducting transition was observed on the resistivity with the onset of superconductivity at 7.4 K and the zero resistance near 6.7 K. Thus the measurements<sup>15</sup> confirmed the superconductivity in the silver boride system. However the observed T<sub>c</sub> was significantly lower than the theoretically predicted value<sup>7,8</sup> and comparable with T<sub>c</sub> for some d metal diborides: ZrB<sub>2</sub> (5.5 K), TaB<sub>2</sub> (9.5 K) and NbB<sub>2</sub> (5.2 K), see<sup>12</sup>.

This discrepancy may be caused by the inhomogeneous structure of the AgB<sub>2</sub> films, in particular by nonstoichiometry of samples. Recently was established<sup>16,17,18</sup>, that some d metal diborides at nonequilibrium conditions may contain a significant amount of metal vacancies (for Nb<sub>1-x</sub>B<sub>2</sub> and Ta<sub>1-x</sub>B<sub>2</sub> up to x ~ 0.48). The band structure calculations<sup>19</sup> showed that the metal vacancies are most likely to appear in diborides with rather weak M-B covalent bonding. Thus it may be expected for metastable AgB<sub>2</sub> the presence of significant concentration of Ag vacancies.

In this paper, we concentrate on the effects of Ag vacancies on the electronic and cohesive properties of silver

TABLE I: Lattice parameters a and c (Å), cell volume V<sub>0</sub> (Å<sup>3</sup>), bulk modulus B<sub>0</sub> (GPa), its pressure derivative B<sub>0</sub>', intra-  $\alpha_a$  and interlayer  $\alpha_c$  (TPa<sup>-1</sup>) linear compressibility for AgB<sub>2</sub>: experiment and theory.

Parameters	Experimental		Theory <sup>a</sup>		
	see <sup>13</sup>		see <sup>7</sup>	see <sup>26</sup>	Our data <sup>b</sup>
a	3.000	3.040 <sup>25c</sup>	2.980	3.000	3.024
c	3.024	3.180 <sup>14</sup>	3.920	3.617	4.085
c/a	1.0800	-	1.3154	1.2051	1.3414
V <sub>0</sub>	25.253	-	30.147	28.188	32.361
B <sub>0</sub>	-	-	-	239	142
B <sub>0</sub> ',	-	-	-	3.20	4.00
$\alpha_a$ <sup>d</sup>	-	-	-	-0.93	-1.35
$\alpha_c$	-	-	-	-2.10	-3.06

<sup>a</sup>FLAPW<sup>7</sup> and LCAO SCF Hartree-Fock<sup>26</sup> calculations

<sup>b</sup>Our calculations - for pressure interval -10  $\div$  +65 GPa

<sup>c</sup>extrapolated from the Vegard relationship for Ag-doped MgB<sub>2</sub>

<sup>d</sup>The mechanical isostatic pressure effect on the lattice constants generally expressed as: a = a<sub>0</sub>(1 +  $\alpha_a$ P) and c = c<sub>0</sub>(1 +  $\alpha_c$ P), where P is the mechanical pressure in GPa,  $\alpha_a$  and  $\alpha_c$  are axial compressibility.

diboride. For this purpose, the band structure of hexagonal AgB<sub>2</sub>, as well as Ag-deficient Ag<sub>1-x</sub>B<sub>2</sub> (x = 0.875 and 0.750) are investigated theoretically using the projected augmented wave (PAW) method in the framework of the density functional theory (the Vienna ab initio simulation package - VASP<sup>20,21,22,23</sup>) with generalized gradient approximation (GGA) for exchange-correlation potential<sup>24</sup>. The silver diboride have the hexagonal crystal structure

(space group P6/mmm) composed of layers of trigonal prisms of Ag atoms in the center of boron atoms, which form the planar graphite-like networks. Both complete and nonstoichiometric  $\text{AgB}_2$  phases were simulated by the 24-atoms supercell ( $\text{Ag}_8\text{B}_{16}$ ). The removing of one silver atom ( $\text{Ag}_7\text{V}^{Ag}\text{B}_{16}$ , where  $\text{V}^{Ag}$  is the silver vacancy) describes the  $\text{Ag}_{0.875}\text{B}_2$  composition. For the  $\text{Ag}_{0.750}\text{B}_2$  composition (supercell  $\text{Ag}_6\text{V}_2^{Ag}\text{B}_{16}$ ) the possible distributions of Ag vacancies are checked. For this purpose two vacancies (in cell) were located at the nearest positions in the Ag sheets, i.e. the alternation of complete and  $\text{V}^{Ag}$  - containing sheets along c-axis is described (case I). Secondly, two vacancies are placed in the neighbor sheets, and the "uniform" distribution of vacancies in a crystal is modeled (case II), Fig. 1. For all systems the structural parameters  $a$  and  $c$  have been optimized.

Let's discuss the data concerning an ideal  $\text{AgB}_2$  phase. Table 1 shows the optimized lattice parameters of  $\text{AgB}_2$  as well as the zero pressure bulk modulus  $B_0$  and its pressure derivative ( $B_0' = dB_0/dP$ ) in comparison with some previous experimental and theoretical results. There is a significant difference between the contraction rates of intra- and inter-planar periodicity: the compressibility in  $\text{AgB}_2$  is strongly anisotropic and the structure is more compressible in the  $z$  direction ( $c=c_0(1-0.00360P)$ ) than in the  $xy$  plane ( $a=a_0(1-0.00106P)$ ) ( $P$  in GPa). Thus, the interlayer linear compressibility exceeds the intralayer linear compressibility about 2.3 times.

The calculated heat of formation ( $\Delta H$ , defined as a difference in the total energies of  $\text{AgB}_2$  with reference to the  $E_{tot}$  of the constituent elements in their stable modifications: fcc-Ag and rhombohedral boron ( $\alpha\text{-B}_{12}$ )) has a small, but negative value (-0.98 eV/f.u.) testifying the possibility of  $\text{AgB}_2$  synthesis. For comparison,  $\Delta H$  for stable refractory 4d metal diborides  $\text{ZrB}_2$  and  $\text{NbB}_2$  were found to be -4.76 and -3.68 eV/f.u., respectively (FLMTO calculations<sup>19</sup>). The cohesive energy ( $E_{coh} \sim 14.1$  eV/f.u.) is also minimal for  $\text{AgB}_2$  in comparison with other 4d metal diborides: 23.4, 24.8 and 19.3 eV/f.u. for  $\text{ZrB}_2$ ,  $\text{NbB}_2$  and  $\text{YB}_2$ <sup>19</sup>. The metastable nature of  $\text{AgB}_2$  is determined by the very weak inter-layer Ag-B and intra-layer Ag-Ag interactions. The bonding picture may be examined using the difference electron densities ( $\Delta\rho$ ), where neutral atomic charge  $\rho^{at}$  densities are subtracted from the crystalline density  $\rho^{cryst}$ , Fig.2. Negative  $\Delta\rho$  around Ag and positive ones around boron indicate a charge transfer from Ag to B. The  $\Delta\rho$  map shows a strongly covalent B-B bonding in the hexagonal boron sheets. On the contrary, the partial ionic type of the inter-plane Ag-B bonding occurs. The in-plane Ag-Ag bonds are insignificant: (i) the near-spherical symmetry of silver  $\Delta\rho$  contours confirm the absence of Ag-Ag covalency; (ii) the ionic interaction between silver ions is repulsive and (iii) the Ag-Ag distance in diboride (3.004 Å) is about 4% higher than in fcc Ag (2.889 Å) i.e. the decrease in metallic-like bonding also occurs.

The electronic band structure of  $\text{AgB}_2$  obtained in our

calculations coincides with the previous results<sup>4,7</sup>. The  $\text{B}2\text{p}$   $\sigma$ -like (in-plane) bands have a small dispersion along  $\Gamma\text{-A-L}$  in the BZ and form the hole Fermi surfaces<sup>4</sup>. The most attractive feature of  $\text{AgB}_2$  is that the  $\text{B}2\text{p}$   $\sigma$ -like bands are more flat than in  $\text{MgB}_2$ , yielding the higher density of states at the Fermi level ( $N(E_F)$ ). We found that  $N(E_F) = 0.90$  states/eVcell, it is about 20% larger than in  $\text{MgB}_2$  ( $N(E_F) = 0.72$  states/eVcell). Calculated densities of states for  $\text{AgB}_2$ ,  $\text{Ag}_{0.875}\text{B}_2$  and  $\text{Ag}_{0.750}\text{B}_2$  are shown in Fig. 3. The occupied Ag 4d bands are located mainly in the region of -5.8 ÷ -3.3 eV. The upper part of conduction band is composed by comparable contributions of Ag 4d and antibonding B 2p states.

Let us consider the effect of silver vacancies on the structural, cohesion and electronic properties of  $\text{AgB}_2$ . The introducing of  $\text{V}^{Ag}$  leads to the reduction of both lattice constants; however for  $x = 0.125$  the  $c/a$  ratio decreases, whereas for  $x = 0.250$  this parameter grows and it appears larger, than that for complete  $\text{AgB}_2$ , Table 2. The inter-planar compression is more pronounced for the "uniform"  $\text{V}^{Ag}$  distribution (model II).

In Table 2 the energies of vacancy formation ( $E_{vf}$ ) as well as  $E_{coh}$  and  $\Delta H$  for  $\text{Ag}_{1-x}\text{B}_2$  phases are summarized. These parameters are calculated as:

$$E_{vf} = E_{tot}^{AgB_2} - E_{tot}^{Ag_{1-x}B_2} - xE_{tot}^{Ag}, \quad (1)$$

$$E_{coh}^{Ag_{1-x}B_2} = E_{tot}^{Ag_{1-x}B_2} - [(1-x)E_{at}^{Ag} + 2E_{at}^B], \quad (2)$$

$$\Delta H^{Ag_{1-x}B_2} = E_{tot}^{Ag_{1-x}B_2} - [(1-x)E_{tot}^{Ag} + 2E_{tot}^B], \quad (3)$$

where  $E_{at}^{Ag}$ ,  $E_{at}^B$  are the total energies of free silver and boron atoms,  $E_{tot}^{Ag}$ ,  $E_{tot}^B$  are the total energies of fcc Ag metal and  $\alpha$ -boron; and  $E_{tot}^{AgB_2}$ ,  $E_{tot}^{Ag_{1-x}B_2}$  are the total energies (per formula units) of  $\text{AgB}_2$  and  $\text{Ag}_{1-x}\text{B}_2$ , respectively.

The calculated vacancy formation energy (0.34 eV) is essentially less than for  $\text{Nb}_{1-x}\text{B}_2$  ( $E_{vf} \sim 1.1$  eV<sup>19</sup>) for which the metal vacancies were found experimentally<sup>16,17,18</sup>. Hence, their presence is very probably and the stoichiometry of  $\text{AgB}_2$  based materials will be very sensitive to the synthesis conditions.

The redistribution of the charge states near  $\text{V}^{Ag}$  is demonstrated in Fig. 2. As is seen, in the Ag-deficient boride the B-B bonds remain almost undistorted. No new bonds going through the vacancy are formed. The difference map shows a weak density accumulation along the  $\text{B} \rightarrow \text{V}^{Ag}$  direction, however the absence of the electron localization on the vacancy clearly follows from  $\Delta\rho$  contour distribution in the planar (100) silver sheet, i.e. the charge states of silver vacancies are close to neutral.

TABLE II: Lattice parameters ( $\text{\AA}$ ), cohesive energies ( $E_{coh}$ ), heat of formation ( $\Delta H$ ) and vacancy formation energies ( $E_{vf}$ ) in eV/f.u. for complete and silver-deficient Ag borides.

Diborides	a	c	c/a	$E_{coh}$	$\Delta H$	$E_{vf}$
AgB <sub>2</sub>	3.024	4.085	1.3414	14.06	-0.98	-
Ag <sub>0.875</sub> B <sub>2</sub>	3.008	4.020	1.3364	13.71	-0.64	0.34
Ag <sub>0.75</sub> B <sub>2</sub> (I) <sup>a</sup>	2.942	3.960	1.3460	13.32	-0.26	0.71 <sup>b</sup>
Ag <sub>0.75</sub> B <sub>2</sub> (II)	2.950	3.950	1.3551	13.35	-0.27	0.70

<sup>a</sup>Models I,II: Ag<sub>0.75</sub>B<sub>2</sub> with various V<sup>Ag</sup> displacement, see Fig.1.  
<sup>b</sup>per two Ag vacancies

In the vicinity of vacancy only insignificant deformation of  $\Delta\rho$  contours appears along the direction Ag  $\rightarrow$  V<sup>Ag</sup>. Figure 3 shows the evolution of the DOS near the Fermi

level with the change of Ag-vacancies concentration in Ag<sub>1-x</sub>B<sub>2</sub>. The Fermi level slightly shifts towards the low energies with increasing x, while the dependence of N(E<sub>F</sub>) is sensitive to vacancy concentration. The N(E<sub>F</sub>) values for Ag<sub>0.875</sub>B<sub>2</sub> and Ag<sub>0.750</sub>B<sub>2</sub> are 0.88 and 0.92 states/eVcell, respectively.

In summary, we presented the results of band structure calculations for silver-deficient AgB<sub>2</sub> performed by the VASP method. It was established that vacancies are likely to appear in AgB<sub>2</sub>: the energy of metal vacancies formation in silver diboride is the least among all 4d metal diborides. Thus, the nonstoichiometry on Ag-sublattice should be easily achievable, i.e. for AgB<sub>2</sub> it is possible to expect the wide homogeneity region. Our analysis indicates that metal vacancies in AgB<sub>2</sub> do not lead to essential reduction of N(E<sub>F</sub>) which seems to be critical in depressing of superconductivity in this system.

#### Acknowledgment.

This work was supported by the RFBR, grant 02-03-32971, and the Russian Foundation for Scientific Schools, grant SS 829.2003.3.

---

<sup>1</sup> J. Nagamatsu, N.Nakagawa, T.Muranaka, Y.Zenitani, and J. Akimitsu, Nature (London), **410**, 63 (2001).  
<sup>2</sup> P. Vajeeston, P. Ravindran, C. Ravi, and R. Asokamani, Phys. Rev., **B63**, 5115 (2001).  
<sup>3</sup> S. Suzuki, S. Higai, and K. Nakao, J. Phys. Soc. Jpn., **70**, 1206 (2001).  
<sup>4</sup> I.R. Shein, N.I. Medvedeva, and A.L. Ivanovskii, Phys. Solid State **43**, 2213 (2001).  
<sup>5</sup> N.I. Medvedeva, A.L. Ivanovskii, J.E. Medvedeva, and A.J. Freeman, Phys. Rev., **B64**, R020502 (2001).  
<sup>6</sup> M.J. Mehl, D. A. Papaconstantopoulos, and S. Singh, Phys. Rev., **B64**, 140509 (2001).  
<sup>7</sup> S.K. Kwon, S.J. Youn, K.S. Kim, and B.I. Min, cond-matter/0106483 (2001).  
<sup>8</sup> F. Yang, R.S. Han, N.H. Tong and W. Guo, Chinese Phys. Lett., **19**, 1336 (2002).  
<sup>9</sup> T. Oguchi, J. Phys. Soc. Jpn., **71**, 1495 (2002).  
<sup>10</sup> I.R. Shein, N.I. Medvedeva, and A.L. Ivanovskii, Phys. Solid State **44**, 1833 (2002).  
<sup>11</sup> G. Profeta, A. Continenza, F. Bernardini, S. Massidda, Phys. Rev., **B65**, art no. 054502 (2002).  
<sup>12</sup> A.L. Ivanovskii, Phys. Solid State, **45**, 1829 (2003).  
<sup>13</sup> V.N. Gurin and M.M. Korsukova, in Boron and Refractory Borides edited by V.I. Matkovich ( Springer-Verlag Berlin Heidelberg New York 1977) p. 301.  
<sup>14</sup> M. Sinder and J. Pelleg, cond-mat/0212632 (2002).  
<sup>15</sup> R. Tomita, H. Koga, T. Uchiyama and I. Iguchi, J. Phys. Soc. Japan, **73**, 2639 (2004).  
<sup>16</sup> A. Yamamoto, C. Takao, T. Masui, M. Izumi and S. Tajima, Physica C, **383**, 197 (2002).  
<sup>17</sup> H. Takeya, A. Matsumoto, K. Hirata, Y.S. Sung and K. Togano, Physica C, **412-414**, 111 (2004).  
<sup>18</sup> H. Takeya, K. Togano, Y. S. Sung, T. Mochiku and K. Hirata, Physica C, **408-410**, 144 (2004).  
<sup>19</sup> I. R. Shein, N. I. Medvedeva, and A. L. Ivanovskii, Phys. Solid State, **45**, 1617(2003).  
<sup>20</sup> G. Kresse, J. Hafner, Phys. Rev., **B47**, 558 (1993).  
<sup>21</sup> G. Kresse, J. Furthmuller, Comput. Mat. Sci., **6**, 15 (1996).  
<sup>22</sup> G. Kresse , J. Furthmuller, Phys. Rev., **B54**, 11169 (1996).  
<sup>23</sup> G. Kresse, J. Joubert, Phys. Rev., **B59**, 1758 (1999).  
<sup>24</sup> J.P. Perdew, K. Burke, M. Ernzerhof, Phys. Rev. Lett., **77**, (1996) 3865.  
<sup>25</sup> C.H. Cheng, Y. Zhao, X.T. Zhu, J. Nowotny, C.C. Sorrell, T. Finlayson and H. Zhang, Physica C, **386**, 588 (2003).  
<sup>26</sup> F. Parvin, A.K.M.A. Islam, F.N. Islam, A.F.M.A. Wahed and M.E. Haque, Physica C, **390**, 16 (2003).

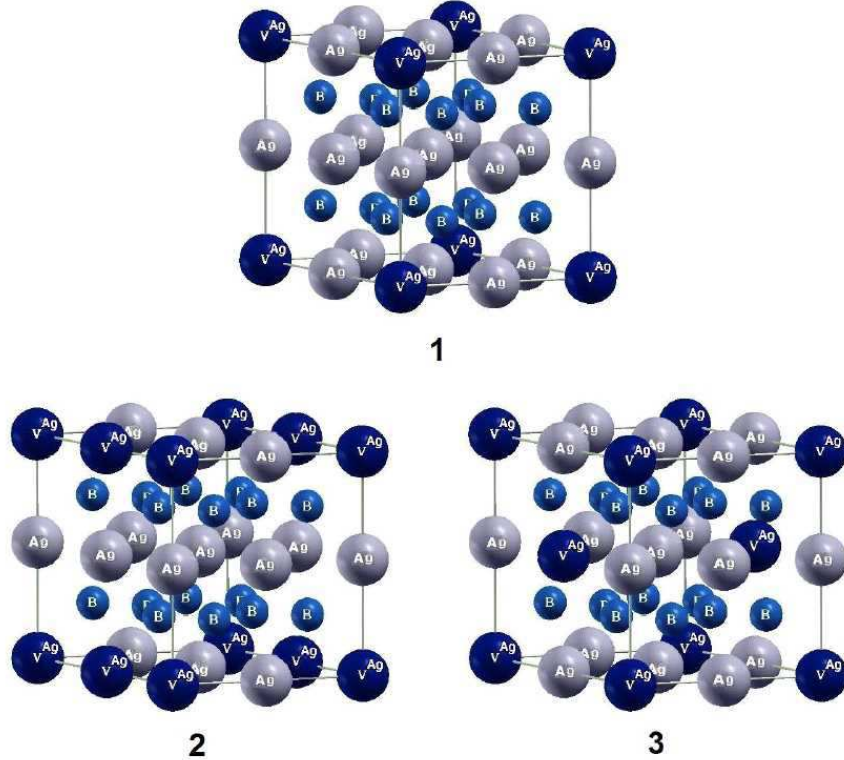


FIG. 1: Fig. 1. Structural models for silver-deficient  $\text{Ag}_{1-x}\text{B}_2$ : 1 -  $\text{Ag}_{0.875}\text{B}_2$  and 2,3 -  $\text{Ag}_{0.750}\text{B}_2$ . The possible distribution of Ag vacancies ( $\text{V}^{\text{Ag}}$ ) are presented: 2 - the alternation of complete and  $\text{V}^{\text{Ag}}$  - containing sheets (along z-axis, model I) and 3 - the "uniform"  $\text{V}^{\text{Ag}}$  distribution (model II), respectively.

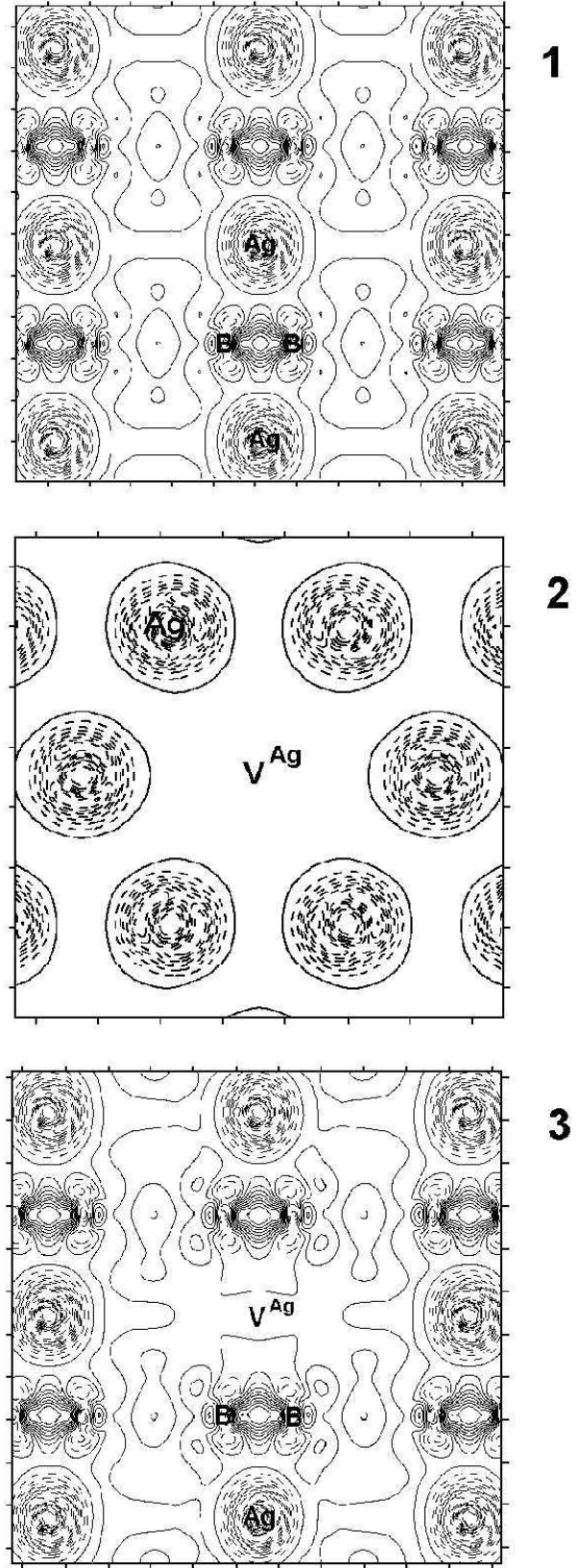


FIG. 2: Fig. 2. Inter-plane charge-density difference ( $\Delta\rho$ ) maps for  $\text{AgB}_2$  (1),  $\text{Ag}_{0.875}\text{B}_2$  (3) and  $\Delta\rho$  map in (100) silver sheet of  $\text{Ag}_{0.875}\text{B}_2$ . In the  $\Delta\rho$  plots, solid and dashed lines indicate an increase and a decrease of the electron density  $\Delta\rho_{\text{AgB}_2}$  relative to the atomic ( $\rho^{\text{Ag}}$ ,  $\rho^{\text{B}}$ ) superposition, respectively.

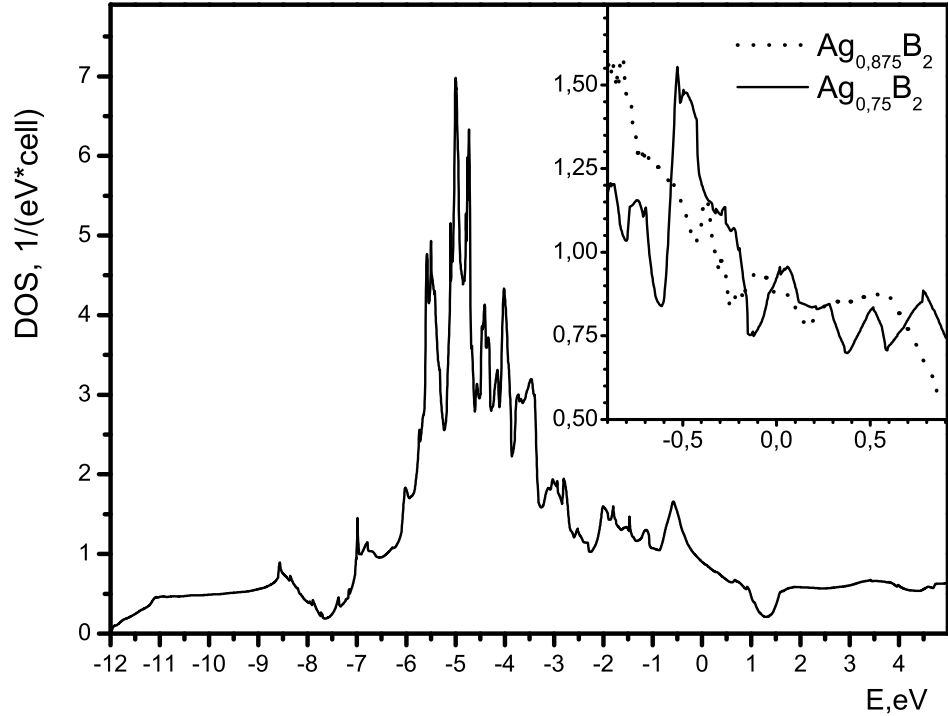


FIG. 3: Density of states for  $\text{AgB}_2$ . *Inset* shows near-Fermi DOSs for  $\text{Ag}_{0.875}\text{B}_2$  and  $\text{Ag}_{0.750}\text{B}_2$ .  $E_F = 0$  eV.